Journal of the Serbian Chemical Society
JSCS-info@shd.org.rs • www.shd.org.rs/JSCS
*J. Serb. Chem. Soc.* 82 (4) 449–463 (2017)
*JSCS–4980*
UDC 546.42'33+666.32:544.723:628.316.12
*Original scientific paper*

# Adsorption of strontium on different sodium-enriched bentonites

SANJA R. MARINOVIĆ[1]*, MARIJA J. AJDUKOVIĆ[1], NATAŠA P. JOVIĆ-JOVIČIĆ[1]**, TIHANA M. MUDRINIĆ[1], BOJANA M. NEDIĆ-VASILJEVIĆ[2], PREDRAG T. BANKOVIĆ[1] and ALEKSANDRA D. MILUTINOVIĆ-NIKOLIĆ[1#]

[1]*University of Belgrade, Institute of Chemistry, Technology and Metallurgy, Njegoševa 12, Belgrade, Serbia and* [2]*University of Belgrade, Faculty of Physical Chemistry, Studentski trg 12–16, Belgrade, Serbia*

(Received 10 October, revised 19 December, accepted 21 December 2016)

*Abstract*: Bentonites from three different deposits (Wyoming, TX, USA and Bogovina, Serbia) with similar cation exchange capacities were sodium enriched and tested as adsorbents for $Sr^{2+}$ in aqueous solutions. X-Ray diffraction analysis confirmed successful Na-exchange. The textural properties of the bentonite samples were determined using low-temperature the nitrogen physisorption method. Significant differences in the textural properties between the different sodium enriched bentonites were found. Adsorption was investigated with respect to adsorbent dosage, pH, contact time and the initial concentration of $Sr^{2+}$. The adsorption capacity increased with pH. In the pH range from 4.0––8.5, the amount of adsorbed $Sr^{2+}$ was almost constant but 2–3 times smaller than at pH ≈11. Further experiments were performed at the unadjusted pH since extreme alkaline conditions are environmentally hostile and inapplicable in real systems. The adsorption capacity of all the investigated adsorbents toward $Sr^{2+}$ was similar under the investigated conditions, regardless of significant differences in the specific surface areas. It was shown and confirmed by the Dubinin–Radushkevich model that the cation exchange mechanism was the dominant mechanism of $Sr^{2+}$ adsorption. Their developed microporous structures contributed to the $Sr^{2+}$ adsorption process. The adsorption kinetics obeyed the pseudo-second-order model. The isotherm data were best fitted with the Langmuir isotherm model.

*Keywords*: $Sr^{2+}$; water purification; Na-enriched clays; cation exchange capacity; textural properties.

*,** Corresponding authors. E-mail: (*)sanja@nanosys.ihtm.bg.ac.rs; (**)natasha@nanosys.ihtm.bg.ac.rs
# Serbian Chemical Society member.
doi: 10.2298/JSC161010008M

## INTRODUCTION

Strontium is abundantly present in the Earth's crust in the form of minerals: $SrCO_3$, $SrSO_4$ and $Al_2O_3{\cdot}SrO{\cdot}(SiO_2)_6{\cdot}4H_2O$. In surface waters, strontium originates from the weathering of rocks or from the discharge of wastewater from industries that use strontium compounds. Ionic strontium is not toxic in small concentrations, and since its concentration in water is generally low, it could be regarded as a harmless substance. The environmental impact of Sr arises from its radioactive isotopes. Besides the four stable Sr isotopes naturally present in soil, there are also artificial, radioactive isotopes $^{89}Sr$ and $^{90}Sr$.[1,2] These radioactive isotopes occur as waste products in nuclear power plants and in the reprocessing of nuclear fuels.[3]

Strontium is an alkaline earth metal that resembles calcium and barium in chemical properties. Due to its similarity with calcium, strontium tends to accumulate in bone tissues in the same manner. In the case of radioactive strontium, accumulation in bone tissue causes radiation damage affecting human and/or animal health.[4] Therefore, the presence of radioactive Sr in the environment should be resolved.

The disposal of radioactive wastewater from commercial nuclear plants is one of the major problems in nuclear waste management.[5] The adsorption of strontium from wastewater prior to its discharge to water bodies in the environment is among the most suitable solutions for pollution prevention.

The adsorption of non-radioactive strontium has been investigated on different adsorbents, such as a PAN/zeolite composite,[6] expanded perlite,[7] activated carbon,[2] *etc*. Some authors investigated the adsorption of radioactive strontium on kaolinite and montmorillonite,[8] illite/smectite mixed clays[9] and on magnetite and a magnetite silica composite.[10]

The adsorptive behavior of radioactive strontium isotopes is similar to that of non-radioactive strontium. This enables the potential adsorptive removal of radioactive strontium from aqueous solutions to be determined using experimental results and models obtained for systems containing the non-radioactive isotopes.

Bentonites are widely used as adsorbents for the removal of heavy metals from wastewater.[11–14] They are low cost, naturally occurring, non-toxic materials, abundantly present in different parts of the world, including Serbia.[12,14–16] Bentonites are clays rich in smectite minerals. Smectites are 2:1 phyllosilicates – layered minerals the layers of which are composed of an octahedral $[AlO_3(OH)_3]^{6-}$ sheet sandwiched between two opposing tetrahedral $[SiO_4]^{4-}$ sheets.[17] Smectites have a total (negative) layer charge between 0.2 and 0.6 per half unit cell and include the tri-octahedral smectites: hectorite, saponite, sauconite, stevensite and swinefordite, and di-octahedral smectites: beidellite, montmorillonite, nontronite and volkonskoite. Beidellite and montmorillonite differ in the origin of the net structural charge. The net structural charge of beidellite is

mainly located in smectite tetrahedral sheets, while that of montmorillonite is mainly located in smectite octahedral sheets.[17]

The present work is focused on the removal of $Sr^{2+}$ from aqueous solutions using three different sodium-enriched bentonites with similar cation exchange capacities (*CEC*) but with different textural properties, particularly different specific surface areas. The bentonites selected for this work included standard source clays from the Clay Minerals Society[18] and a previously well-characterized clay from a Serbian deposit.[19,20] The adsorption was studied as a function of adsorbent dosage, suspension pH, adsorption time and the initial concentration of $Sr^{2+}$. The goal of this investigation was to confirm the applicability of the investigated bentonites as $Sr^{2+}$ adsorbents and to determine the most significant adsorption mechanism for $Sr^{2+}$.

## EXPERIMENTAL

### *Materials*

Two bentonites were supplied by the Clay Minerals Society: a Ca-montmorillonite dominant clay (STx-1) originating from the Manning Formation, County of Gonzales, Texas, USA and a Na-montmorillonite dominant clay (SWy-2) originating from the Newcastle Formation in the County of Crook, Wyoming, USA.[18] The chemical composition (mass %) of STx-1 was: $SiO_2$, 70.1; $Al_2O_3$, 16.0; $TiO_2$, 0.22; $Fe_2O_3$, 0.65; FeO, 0.15; MnO, 0.009; MgO, 3.69; CaO, 1.59; $Na_2O$, 0.27; $K_2O$, 0.078; F, 0.084; $P_2O_5$, 0.026; S, 0.04 and $CO_2$, 0.16 and ignition loss up to 1100 °C was 6.54 mass %. The composition of SWy-2 was: $SiO_2$, 62.9; $Al_2O_3$, 19.6; $TiO_2$, 0.090; $Fe_2O_3$, 3.35; FeO, 0.32; MnO, 0.006; MgO, 3.05; CaO, 1.68; $Na_2O$, 1.53; $K_2O$, 0.53; F, 0.111; $P_2O_5$, 0.049; S, 0.05 and $CO_2$, 1.33, and the ignition loss up to 1100 °C was 6.06 mass %.[18]

The third bentonite material (the dominant smectite mineral phase of which consisted of montmorillonite and beidellite in the ratio of approx. 1:9)[21] was obtained from the "Bogovina Coal and Bentonite Mine", Bogovina, Serbia. It had been previously thoroughly characterized[19,22] and tested as a Pb, Cd and Ni adsorbent.[23] The chemical composition (mass %) of this clay was: $SiO_2$, 57.51; $Al_2O_3$, 17.13; $Fe_2O_3$, 7.67; MgO, 2.35; CaO, 1.81; $Na_2O$, 0.75; $K_2O$, 1.18 and $CO_2$, 0.5, and the ignition loss was 11.10 mass %.[19]

As previously reported, the cation exchange capacities (*CEC*) of the bentonites obtained by the ammonium acetate method[24] were 84.4, 76.4 and 63.3 mmol of monovalent cation per 100 g of clay dried at 110 °C for the Texas, Wyoming and Bogovina originating bentonites, respectively.[18,20]

The samples were sieved through a 74-μm sieve. Sodium enrichment of the bentonite samples was performed using the previously reported procedure[20] and the obtained materials based on Wyoming, Texas and Bogovina bentonites were denoted as Na-W, Na-T and Na-B, respectively. Sodium enrichment was performed with the goal of obtaining homoionic absorbents with $Na^+$ as the exchangeable cation, which could be more easily replaced with $Sr^{2+}$ in the adsorption process.

$SrCl_2 \cdot 6H_2O$, with 98 % purity, was obtained from Carlo Erba and used as received.

*Characterization methods*

The X-ray diffraction patterns of the powders of Na-enriched bentonites were obtained using a Philips PW 1710 X-ray powder diffractometer, equipped with a Cu anode ($\lambda$ = = 0.154178 nm).

The point of zero charge ($pH_{PZC}$) was determined using a batch equilibration technique.[25] Suspensions each containing 50 mg of one of the bentonite samples in 20 $cm^3$ of a $10^{-2}$ mol $dm^{-3}$ NaCl solution were prepared by shaking for 24 h at room temperature. The initial pH values ($pH_i$) were adjusted in the pH range from 2 to 12 by the addition of small amounts of 0.1 mol $dm^{-3}$ HCl or NaOH solution. The $pH_i$ and $pH_f$ (final pH measured after 24 h of shaking) were measured using a Meterlab pH/ION Meter PHM240 pH-meter. The point of zero charge was determined from the $pH_i$ *vs*. $pH_f$ diagram.

Nitrogen physisorption isotherms were determined on a Thermo Finnigan Sorptomatic 1990 instrument at –196 °C and the values of the textural parameters were obtained using the ADP 2005 software. The samples were out-gassed at 160 °C for 20 h. Textural parameters' values were calculated according to the usual methods.[26-28] The specific surface area, $S_{BET}$, was calculated from the adsorption data in the $p/p_0$ range from 0.05 to 0.26 according to the Brunauer, Emmett, Teller method. The total pore volume, $V_{0.98}$, was calculated according to the Gurvitsch method. The Dubinin–Radushkevich method was used for the calculation of the micropore volume, while specific surface area in the micropore region was obtained using the Horvath–Kawazoe method. Pore diameter distribution curves were obtained according to the Barrett, Joyner, Halenda method. To distinguish between micropores and the external surface area, the *t*-plot method was applied. The Harkins and Jura relation was used as the standard reference *t*-curve.

*Adsorption experiments*

Batch-type adsorption experiments were conducted in aqueous solutions in a temperature-controlled water bath shaker (Memmert WNE 14 and SV 1422). Adsorption was carried out with respect to contact time and initial $Sr^{2+}$ concentration.

Aliquots were withdrawn from the shaker at regular time intervals and the solution was centrifuged at 17000 rpm for 10 min (Hettich EBA-21). The $Sr^{2+}$ content in the supernatant solutions was determined by inductively coupled plasma optical emission spectrometry (ICP– –OES). The strontium concentrations in the supernatants were determined using an iCAP 6500 Duo ICP (Thermo Fisher Scientific, Cambridge, UK) inductively coupled plasma optical emission spectrometer (ICP-OES) with iTEVA operational software. The strontium calibration solutions were prepared using multi-element plasma standard solution 4, Specpure® (Alfa Aesar, Germany). Strontium concentration was measured at the emission wavelength Sr II 215.284 nm. For each sample, the measurement was performed in triplicate. The relative standard deviation was lower than 0.5 %. Analytical process quality control was performed using a certified reference material (EPA method 200.7 LPC solution; ULTRA Scientific, USA), which indicated a strontium recovery of 99.4 %.

All experiments were performed in triplicate at 25 °C, using the same mass of adsorbent ($m_{ads}$ = 20.0 mg) and volume of solution ($V$ = 50.0 $cm^3$). The amount of $Sr^{2+}$ adsorbed $q_t$ (mg $g^{-1}$) after time $t$ was calculated from the following mass balance relationship:

$$q_t = \frac{c_0 - c_t}{m_{ads}} \tag{1}$$

where $c_0$ and $c_t$ are the concentration (mg dm$^{-3}$) of $Sr^{2+}$ in solution initially and after adsorption time $t$, respectively.

## RESULTS AND DISCUSSION

### *X-Ray powder diffraction*

The XRD patterns of the powders of the Na-enriched bentonites are presented in Fig. 1.

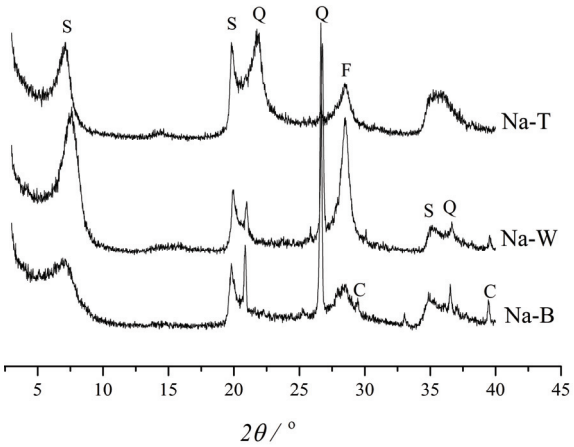


Fig. 1. The XRD patterns of the powders of the Na-enriched bentonites (S – smectite, Q – quartz, F – feldspar and C – calcite).

The obtained diffractograms confirmed the phase composition of bentonites with dominant smectite phase (either montmorillonite or a montmorillonite/beidelite mixture) with different associated minerals in accordance with the different origins of the bentonites. As expected, Na-W contained the highest amount of feldspar among the investigated bentonites, while Na-B had the highest amount of quartz.[22,29] Only Na-B contained a detectable amount of calcite as an impurity. The XRD pattern revealed that Na-exchange had been successfully performed since the position of the 001 smectite peak in all the investigated samples corresponded to the Na-forms of smectite with $d_{001}$ at around 1.2–1.3 nm.[30] The raw bentonites from Texas and Bogovina were dominantly smectites of the Ca--type with characteristic basal spacing of $d_{001}$ = 1.5 nm.

### *Textural properties*

Low temperature $N_2$ physisorption measurements resulted in the isotherms presented in Fig. 2.

All the presented isotherms were reversible at lower equilibrium pressures, belonging to the type II isotherms according to IUPAC nomenclature. Type II isotherms are characteristic for materials consisting of aggregated planar particles that form slit shape pores. Such a result is in accordance with the literature.[31] At equilibrium pressures above $p/p_0$ = 0.4, a hysteresis loop of the H3 type appeared,

which indicates multilayer nitrogen adsorption and capillary condensation within the smectite mesopores of all the smectites.[22,32] The adsorption isotherms of all the materials exhibited an inflection point at about $p/p_0 = 0.2$. This indicates that no overlapping between monolayer and multilayer adsorption occurred, *i.e.*, the formation of the second adsorption layer began only after monolayer adsorption had been completed. Selected textural data are presented in Table I.

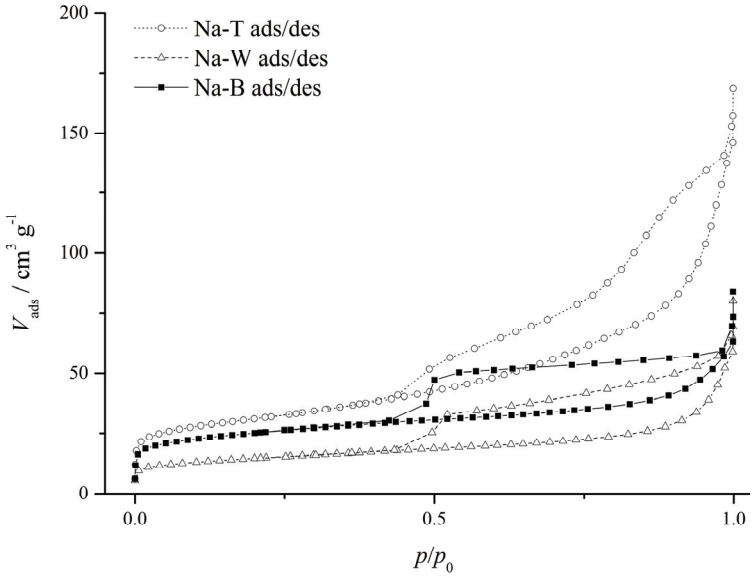


Fig. 2. Nitrogen adsorption–desorption isotherms of Na-T, Na-W and Na-B.

TABLE I. Selected textural properties; $S_{BET}$ – specific surface area (Brunauer, Emmett, Teller – three parameter plot); $V_{0.98}$ – total pore volume (Gurvitch); $V_{mes,BJH}$ – mesopore volume (Barrett, Joyner, Hallenda); $d_{med}$ – median pore diameter; $d_{max}$ – the most abundant pore diameter; $S_t$ – specific surface area (*t*-plot); and $S_{mic}$ – micropore specific surface area

| Sample | $S_{BET}$ m$^2$ g$^{-1}$ | $V_{0.98}$ cm$^3$ g$^{-1}$ | $V_{mes,BJH}$ cm$^3$ g$^{-1}$ | $d_{max}$ nm | $d_{med}$ nm | $S_t$ m$^2$ g$^{-1}$ | $S_{mic}=S_{BET}-S_t$ m$^2$ g$^{-1}$ |
|---|---|---|---|---|---|---|---|
| Na-T | 113 | 0.2000 | 0.2101 | 3.83 | 9.17 | 83 | 30 |
| Na-W | 52 | 0.0759 | 0.0871 | 4.08 | 4.26 | 31 | 21 |
| Na-B | 98 | 0.0853 | 0.0788 | 3.93 | 3.99 | 43 | 55 |

All the Na-enriched materials exhibited meso- and microporosity developed to different extents. While the mesoporous surface area increased in the order Na-W < Na-B < Na-T, the increase of the surface area of micropores followed the sequence Na-W < Na-T < Na-B. The microporous surface area should be considered as more relevant in the investigated cation exchange process, since it occurs in the interlamellar smectite region. Therefore, if $Sr^{2+}$ adsorption on the

Na-enriched clays is dominantly dependent on the surface area, the efficiency of $Sr^{2+}$ uptake is expected to follow the sequence Na-B > Na-T > Na-W.

*The effect of adsorbent dosage on the adsorption of $Sr^{2+}$*

In order for the influence of the adsorbent dosage on the adsorption of $Sr^{2+}$ ions to be investigated, the mass of all investigated Na-enriched bentonites was varied from 10 to 100 mg. All the experiments were performed for three hours at 25 °C with an initial $Sr^{2+}$ concentration of 50 mg $dm^{-3}$.

The influence of adsorbent dosage on the amount of $Sr^{2+}$ ions adsorbed on the investigated Na-enriched bentonites after 180 min at 25 °C is presented in Fig. 3.

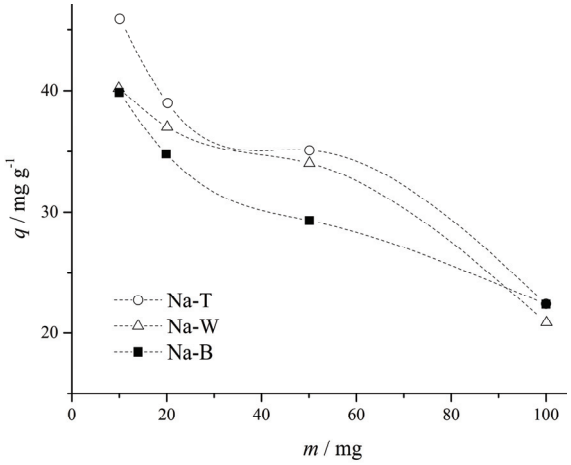


Fig. 3. The influence of adsorbent dosage on the amount of adsorbed $Sr^{2+}$.

As expected, the quantity of adsorbed $Sr^{2+}$ per unit mass of adsorbent decreased with increasing adsorbent dosage. It decreased steeply from a dosage of 10 mg to one of 20 mg, after which a plateau was attained. For dosages from 20 to 50 mg, the adsorption per unit mass did not change significantly. After the plateau, the drop in the adsorption per unit mass was more pronounced.

For a dosage of 100 mg, almost complete $Sr^{2+}$ removal was obtained. A dosage of 20 mg was chosen because it is in the plateau of the *q*–*m* diagram, while it is low enough to meet economic requirements.

*The effect of pH on the adsorption of $Sr^{2+}$*

The effect of the initial pH on the adsorption of $Sr^{2+}$ was investigated within the pH range 2–11 and the results are presented in Fig. 4, together with the pH behavior of all the Na-enriched bentonites.

The diagram shows the initial pH of the suspensions of Na-enriched bentonites in 0.01 M NaCl ($pH_i$) *vs*. pH after 24 h of shaking ($pH_f$). A plateau

between pH values of 4 and 8.5 was observed and the point of zero charge ($pH_{PZC}$) was estimated to be 6.5 for Na-T, 6.3 for Na-W and 8.2 for Na-B.

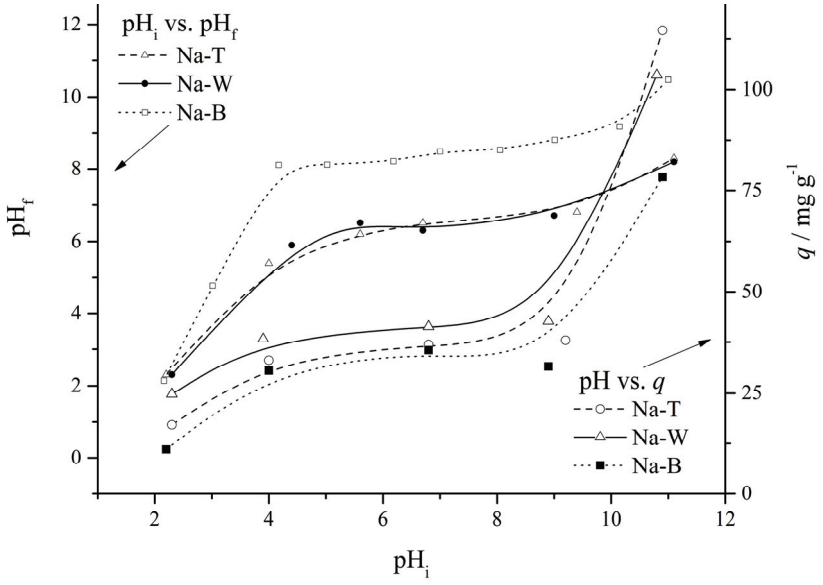


Fig. 4. The effect of pH on the adsorption of $Sr^{2+}$ and $pH_i$ *vs.* $pH_f$ diagram.

Lower than $pH_{PZC}$, the surface charge of the samples is positive, while above these values, the surface charge is negative. On the other hand, strontium is in the cationic form within the entire investigated pH range.

The quantity of adsorbed $Sr^{2+}$ was very low in an extremely acidic environment, which could be explained by the repulsion between positive surface charge of the adsorbents and $Sr^{2+}$. In the 4–8.5 pH range, the amount of adsorbed $Sr^{2+}$ was higher and almost constant due to a constant ratio between the positive and negative surface charges of the adsorbents. Further increases of the pH value (>8.5) led to very high amounts of adsorbed $Sr^{2+}$ as a consequence of the electrostatic interaction of the negative surface of adsorbents and the $Sr^{2+}$.

Further experiments were realized at an unadjusted pH (pH 6.8), which lies on the plateau in Fig. 4, where the adsorption efficiency is almost constant in the pH interval from 4 to 8.5.[33] Unadjusted pH was also chosen because adjusting the pH would lead to an additional operation, which increases the procedure cost. Moreover, extreme pH values could cause ecological problems that should be avoided. The adsorption at unadjusted pH was satisfactory (around 30 % removal of $Sr^{2+}$ from water) under the given experimental conditions.[34]

*The effect of contact time on the adsorption of $Sr^{2+}$*

In order to determine the equilibrium time for the maximum uptake of $Sr^{2+}$, the adsorption of $Sr^{2+}$ was monitored with respect to contact time. The initial $Sr^{2+}$ concentration was 50 mg $dm^{-3}$.

The effect of contact time on the amount of $Sr^{2+}$ adsorbed on the bentonites is presented in Fig. 5.

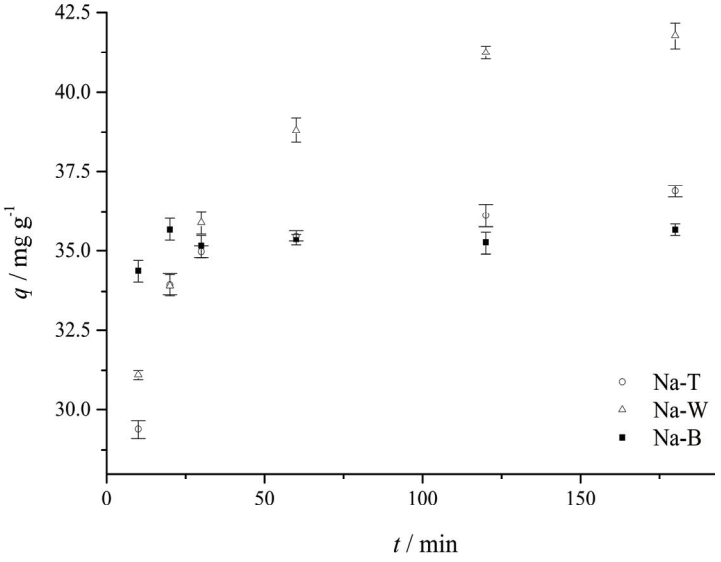


Fig. 5. The effect of contact time on the adsorption of $Sr^{2+}$ on the three studied bentonites.

For all adsorbents, adsorption rate was initially high and then, it gradually reached a plateau. All adsorbents exhibited similar $t_{1/2}$ values ($t_{1/2}$ – the time at which the amount of adsorbed $Sr^{2+}$ is equal to half of the total amount adsorbed at equilibrium). The $t_{1/2}$ values were 5.8, 6.9 and 5.5 min for Na-T, Na-W and Na-B, respectively. Both parameters that describe adsorbent quality, *i.e.*, the amount of $Sr^{2+}$ adsorbed per unit mass and $t_{1/2}$, were similar for all the sodium-enriched bentonites. The obtained results confirmed that the degree of the development of a porous structure had no influence on the adsorption of $Sr^{2+}$. Na-W, the material with the least developed micro and mesopore surface, even exhibited a slightly higher adsorption of $Sr^{2+}$. This indicates that the ion exchange mechanism was the dominant adsorption mechanism.

The pseudo-first order and pseudo-second order kinetics models were tested for the adsorption of $Sr^{2+}$ on the Na-enriched bentonites.

The parameters calculated for the pseudo-first and pseudo-second order kinetics models[35,36] are presented in Table II.

TABLE II. Pseudo-first-order-kinetics and pseudo-second-order-kinetics for the adsorption of $Sr^{2+}$ ions on Na-T, Na-W and Na-B; $k_1$ is the pseudo-first order rate constant; $k_2$ is the pseudo-second order rate constant; $q_e^{exp}$ is the experimentally obtained value for the equilibrium adsorption capacity; $q_e^{calc}$ is calculated value for the equilibrium adsorption capacity and $R^2$ is the square of the correlation coefficients

| Sample | Na-T | Na-W | Na-B |
|---|---|---|---|
| $q_e^{exp}$ / mg g$^{-1}$ | 38.98 | 41.78 | 35.68 |
| Pseudo-first order kinetics model | | | |
| $q_e^{calc}$ / mg g$^{-1}$ | 3.121 | 2.239 | 1.374 |
| $k_1$ / min$^{-1}$ | 0.027 | 0.007 | 0.029 |
| $R^2$ | 0.9978 | 0.6747 | 0.6759 |
| Pseudo-second order kinetics model | | | |
| $q_e^{calc}$ / mg g$^{-1}$ | 37.22 | 42.94 | 35.62 |
| $k_2 \times 10^2$ / g mg$^{-1}$ min$^{-1}$ | 1.092 | 0.447 | 7.269 |
| $R^2$ | 0.9998 | 0.9998 | 0.9999 |

The square of the correlation coefficients ($R^2$) for the pseudo-first order kinetics model were relatively low for Na-W and Na-B, indicating poor correlation of the data with the model. On the other hand, the $R^2$ values for the pseudo--second order kinetics model were > 0.999 for all bentonites. Although Na-T exhibited a rather high $R^2$ value for the pseudo-first order kinetics, the values of the equilibrium adsorption capacity $q_e^{calc}$ calculated from the equation for the pseudo-first order kinetics for all samples exhibited high discrepancy from the experimentally obtained adsorption capacity, $q_e^{exp}$. On the other hand, for the pseudo-second order kinetics model, $q_e^{calc}$ and $q_e^{exp}$ were in good agreement, confirming that the adsorption of $Sr^{2+}$ on the studied bentonites obeyed pseudo--second order kinetics.

The pseudo-second-order kinetics model for the adsorption of $Sr^{2+}$ on the investigated bentonites is shown in Fig. 6.

*The effect of the initial concentration of $Sr^{2+}$ on their adsorption*

The effect of the initial concentration of $Sr^{2+}$ on the adsorption capacity was also investigated for four different initial concentrations of $Sr^{2+}$ in the concentration range from 25 to 100 mg dm$^{-3}$. The obtained data were fitted using the Langmuir, Freundlich and Dubinin–Radushkevich isotherm models.[37–39]

The value obtained for the adsorption energy could be used to predict the type of adsorption.[40] If $E$ is smaller than 8 kJ mol$^{-1}$, the adsorption could be described as physisorption, while $E$ in the range from 8−16 kJ mol$^{-1}$ indicates chemisorption.

Average values of repeated experiments for each adsorbent were fitted using the Langmuir and Freundlich models and the results are presented in Figs. 7a and b, respectively. The calculated parameters for the investigated models are presented in Table III.

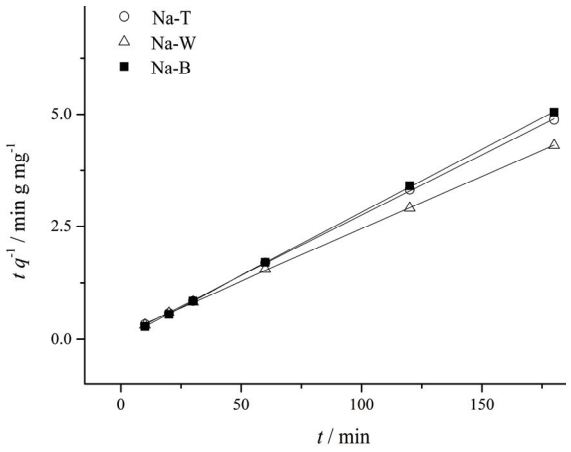


Fig. 6. Plots of the pseudo-second-order kinetics model for the adsorption of $Sr^{2+}$ on the studied bentonites.

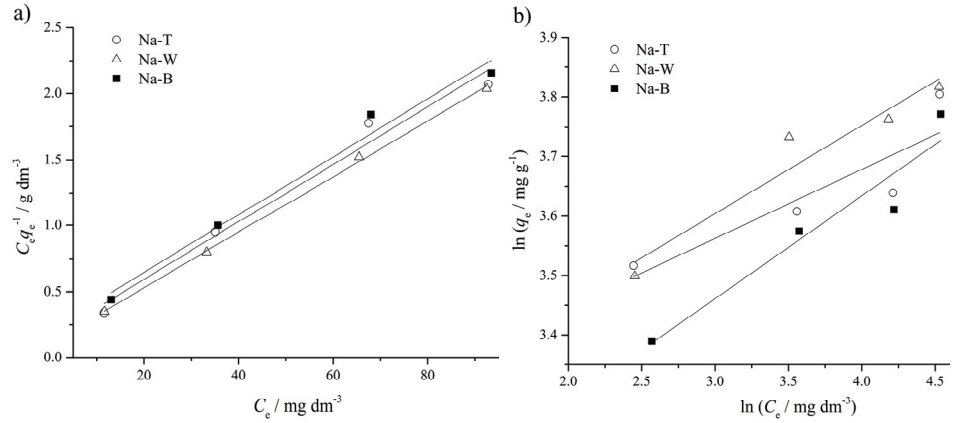


Fig. 7. Adsorption isotherms: a) Langmuir and b) Freundlich isotherm model.

The Langmuir model better fitted the experimental data, having $R^2$ close to unity. It is appropriate to describe the adsorption of $Sr^{2+}$ on all the studied bentonites.

As previously stated, the ion exchange mechanism could be regarded as the dominant adsorption mechanism. In order to verify this statement, the $q_{max}$ values calculated according to the Langmuir model were compared with the corresponding cation exchange capacity (*CEC*) values.[18,20] Since strontium is divalent and the *CEC* values are given for monovalent cations, the $q_{max}$ values should be compared with half of the *CEC* values. The corresponding values were as follows: for Na-T, $q_{max}$ was 0.526 mmol g$^{-1}$ and half the *CEC* value was 0.422 mmol g$^{-1}$; for Na-W, $q_{max}$ was 0.543 mmol g$^{-1}$ and half of the *CEC* value was 0.382 mmol g$^{-1}$ and for Na-B, $q_{max}$ was 0.521 mmol g$^{-1}$ and half of the *CEC* value was 0.316 mmol g$^{-1}$. The obtained values of $q_{max}$ exceeded the

amount of available exchangeable cations, indicating that although the ion exchange mechanism was dominant, there are other contributions to the adsorption process. Bearing in mind that the increase in the surface area of the micropores followed the sequence Na-W < Na-T < Na-B, it could be assumed that developed microporous structure contributed somewhat to the $Sr^{2+}$ adsorption process.

TABLE III. Parameters calculated for the Langmuir, Freundlich and Dubinin–Radushkevich isotherm models; $q_{max}$ is the maximum adsorption capacity; $K_L$ is the Langmuir adsorption constant; $K_F$ and $n$ are the Freundlich adsorption constants characteristic for the system; $K_{DR}$ is the adsorption energy constant and $E$ is the energy of adsorption

| Sample | Na-T | Na-W | Na-B |
|---|---|---|---|
| | Langmuir isotherm | | |
| $q_{max}$ / mg g$^{-1}$ | 46.1 | 47.6 | 45.7 |
| $K_L$ / dm$^3$ mg$^{-1}$ | 7.31 | 5.21 | 9.49 |
| $R^2$ | 0.968 | 0.998 | 0.973 |
| | Freundlich isotherm | | |
| $N$ | 8.62 | 9.558 | 5.78 |
| $K_F$ / dm$^3$ mg$^{-1}$ | 24.9 | 26.6 | 19.0 |
| $R^2$ | 0.689 | 0.901 | 0.880 |
| | Dubinin–Radushkevich | | |
| $K_{DR}$ / mol$^2$ kJ$^{-2}$ | $6.81 \cdot 10^{-3}$ | $6.99 \cdot 10^{-3}$ | $7.43 \cdot 10^{-3}$ |
| $E$ / kJ mol$^{-1}$ | 8.57 | 8.46 | 8.20 |
| $R^2$ | 0.995 | 0.956 | 0.935 |

The squared correlation coefficients ($R^2$) showed that the experimental data were in good agreement with the Dubinin–Radushkevich isotherm model (Table III). The calculated $E$ values were similar for all investigated adsorbents and slightly higher than 8 kJ mol$^{-1}$, indicating that the type of adsorption was chemisorption. According to literature data, the obtained $E$ values were in the range of adsorption energy (8–16 KJ mol$^{-1}$) characteristic for systems where ion exchange is the dominant mechanism.[41]

Since the experiments related to $Sr^{2+}$ adsorption on various adsorbents reported in literature were performed under different experimental conditions, direct comparison of the obtained data is not possible. However, a few descriptive data will be given. Chegrouche *et. al*.[2] reported a maximum adsorption capacity of 0.507 mmol g$^{-1}$ (44.4 mg g$^{-1}$) on activated carbon, while Yusan and Erenturk[6] obtained a maximum adsorption capacity of 0.011 mg g$^{-1}$ on a PAN/ /zeolite composite adsorbent. Ahmadpour *et al*.[5] investigated adsorption of $Sr^{2+}$ on treated almond green hull and obtained a maximum adsorption capacity of 116.3 mg g$^{-1}$. Considering the literature data, the adsorption of $Sr^{2+}$ on the investigated Na-enriched bentonites showed that they could be considered as possible adsorbents for the removal of $Sr^{2+}$ from wastewater.

## CONCLUSIONS

Three different bentonites were sodium-enriched in order to be tested as adsorbents for $Sr^{2+}$. The characterization of these bentonites included XRD and detailed textural analysis. The XRD analysis revealed that Na-exchange had been successfully performed. The mesoporous surface area increased in the order Na-W < Na-B < Na-T, while the increase in the surface area of the micropores followed the sequence Na-W < Na-T < Na-B. The surface areas of the investigated bentonites differed significantly. The adsorption of $Sr^{2+}$ ions from aqueous solutions was performed on all three Na-enriched bentonites. Adsorption was realized with respect to the adsorbent dosage, pH, contact time and initial concentration of $Sr^{2+}$. The adsorption capacity increased with pH. In the pH range from 4–8.5, the amount of adsorbed $Sr^{2+}$ was almost constant but 2–3 times smaller than maximal obtained at pH ≈11. It is concluded that the adsorption was mainly governed by the ion exchange mechanism, since the bentonites with similar *CEC* values and different specific surface areas had similar adsorption capacities. Bearing in mind that the increase of the surface area of micropores followed the sequence Na-W < Na-T < Na-B, it could be assumed that the developed microporous structure contributed somewhat to the $Sr^{2+}$ adsorption process.

The adsorption dynamics was described well by the pseudo-second-order kinetics model. The Langmuir isotherm model best fitted the experimental data. The Dubinin–Radushkevich isotherm was used to provide a better understanding of the adsorption mechanism and to distinguish physisorption from chemisorption. The value obtained for the adsorption energy was slightly higher than 8 kJ $mol^{-1}$. This indicated chemisorption and partially ion exchange as the dominant mechanisms. All the investigated adsorbents could be used for the removal of radioactive strontium, considering the fact that it has similar adsorptive behavior to its non-radioactive counterpart. Moreover, according to the findings in this study, bentonite from unexploited deposits could be used as a $Sr^{2+}$ adsorbent. Knowing the cation exchange capacity of any clay, the prediction of its adsorption potential is possible.

*Acknowledgement.* This work was supported by the Ministry of Education, Science and Technological Development of the Republic of Serbia (Project III 45001).

ИЗВОД

## АДСОРПЦИЈА СТРОНЦИЈУМА НА РАЗЛИЧИТИМ НАТРИЈУМОМ ИЗМЕЊЕНИМ БЕНТОНИТИМА

САЊА Р. МАРИНОВИЋ[1], МАРИЈА Ј. АЈДУКОВИЋ[1], НАТАША П. ЈОВИЋ-ЈОВИЧИЋ[1] , ПРЕДРАГ Т. БАНКОВИЋ[1], ТИХАНА М. МУДРИНИЋ[1], БОЈАНА М. НЕДИЋ ВАСИЉЕВИЋ[2] и АЛЕКСАНДРА Д. МИЛУТИНОВИЋ-НИКОЛИЋ[1]

*[1]Универзитет у Београду – Институт за хемију, технологију и металургију, Центар за катализу и хемијско инжењерство, Његошева 12, Београд и [2]Универзитет у Београду – Факултет за физичку хемију, Студентски трг 12–16, Београд*

Бентонити из три различита налазишта (Вајоминг и Тексас, САД, и Боговина) са сличним капацитетима катјонске измене натријумски су измењени и испитани као

адсорбенси за уклањање $Sr^{2+}$ из водених раствора. Успешност натријумске измене потврђена је рендгено-структурном анализом. Текстурална својства бентонитних узорака су одређена коришћењем методе нискотемпературне физисорпције азота. Добијене су значајне разлике у текстуралним својствима натријумски измењених бентонита различитог порекла. Испитиван је утицај масе адсорбента, pH, времена контакта и почетне концентрације $Sr^{2+}$ на адсорпцију $Sr^{2+}$. Адсорпциони капацитет расте са порастом pH. У опсегу pH од 4 до 8,5 количина адсорбованих $Sr^{2+}$ је скоро константна, али 2 до 3 пута мања од максималне остварене при pH ≈11. У свим наредним експериментима коришћен је неподешени pH раствора, јер је коришћење екстремно базних услова штетно за животну средину и сходно томе неприменљиво у реалним системима. Утврђено је да је адсорпциони капацитет свих адсорбенаса према $Sr^{2+}$ сличан, без обзира на значајне разлике у специфичним површинама. Показано је да је механизам катјонске измене доминантан механизам при адсорпцији $Sr^{2+}$ на натријумски измењеним бентонитима, што је потврђено и моделом Dubinin–Radushkevich. Развијена микропорозна структура такође у извесној мери доприноси процесу адсорпције $Sr^{2+}$. Адсорпциона динамика прати кинетички модел псеудо-другог реда за све адсорбенсе, док Лангмирова изотерма најбоље описује адсорпцију у испитаним системима.

(Примљено 10. октобра, ревидирано 19. децембра, прихваћено 21. децембра 2016)

## REFERENCES

1. J. R. Dojlido, G. A. Best, *Chemistry of water and water pollution*, Ellis Horwood, Chichester, 1993, p. 75
2. S. Chegrouche, A. Mellah, M. Barkat, *Desalination* **235** (2009) 306
3. S. Yusan, S. Erenturk, *World J. Nucl. Sci. Technol.* **1** (2011) 6
4. A. Horr, *Chemistry of strontium in natural water*, U.S. Government. Print. Off, Washington, DC, 1962, p. 4
5. A. Ahmadpour, M. Zabihi, M. Tahmasbi, T. Rohani Bastami, *J. Hazard. Mater*. **182** (2010) 552
6. S. Yusan, S. Erenturk, *World J. Nucl. Sci. Technol.* **1** (2011) 6
7. M. Torab-Mostaedi, A. Ghaemi, H. Ghassabzadeh, M. Ghannadi-Maragheh, *Can. J. Chem. Eng.* **89** (2011) 1247
8. H. N. Erten, S. Aksoyoglu, S. Hatipoglu, H. Göktürk, *Radiochim. Acta* **44/45** (1988) 147
9. T. Missana, M. Garcia-Gutierrez, U. Alonso, *Phys. Chem. Earth* **33** (2008) S156
10. A. Ebner, J. Ritter, J. Navratil, *Ind. Eng. Chem. Res.* **40** (2001) 1615
11. M. K. Uddin, *Chem. Eng. J.* **308** (2017) 438
12. Y. Bentahar, C. Hurel, K. Draoui, S. Khairoun, *Appl. Clay Sci.* **119** (2016) 385
13. M. Cruz-Guzman, R. Celis, M. C. Hermosin, W. C. Koskinen, E. A. Nater, J. Cornejo, *Soil Sci. Soc. Am. J.* **70** (2006) 215
14. R. Yua, S. Wanga, D. Wangb, J. Keb, X. Xinga, N. Kumadac, N. Kinomurac, *Catal. Today* **139** (2008) 135
15. L. Aloui, F. Ayari, A. Ben Othman, M. Trabelsi-Ayadi, *Int. J. Eng. Appl. Sci.* **2** (2015) 33
16. F. Ayari, E. Srasra, M. Trabelsi-Ayadi, *Desalination* **185** (2005) 391
17. F. Bergaya, G. Lagaly, *Developments in Clay Science*, in *Handbook of Clay Science*, Vol. 5A, 2nd ed., Elsevier, Amsterdam, 2013
18. Clay Minerals Society, Source Clay Physical/Chemical Data, http://www.clays.org/ /Sourceclays.html (August 1, 2016)
19. Z. Vuković, A. Milutinović-Nikolić, Lj. Rožić, A. Rosić, Z. Nedić, D. Jovanović, *Clays Clay Miner.* **54** (2006) 697

20. N. Jović-Jovičić, A. Milutinović-Nikolić, M. Žunić, Z. Mojović, P. Banković, I. Gržetić, D. Jovanović, *J. Contam. Hydrol.* **150** (2013) 1
21. T. Novaković, Lj. Rožić, S. Petrović, A. Rosić, *Chem. Eng. J.* **137** (2008) 436
22. Z. Vuković, A. Milutinović-Nikolić, J. Krstić, A. Abu-Rabi, T. Novaković, D. Jovanović, *Mater. Sci. Forum* **494** (2005) 339
23. N. Jović-Jovičić, A. Milutinović-Nikolić, M. Žunić, Z. Mojović, P. Banković, B. Dojčinović, A. Ivanović-Šašić, D. Jovanović, *J. Serb. Chem. Soc.* **79** (2014) 253
24. US Environmental Protection Agency, Method 9080 - *Cation exchange capacity of soils (ammonium acetate)*, USEPA, Washington, DC, 1986, https://www.epa.gov/sites/production/files/2015-12/documents/9080.pdf
25. Lj. Čerović, S. K. Milonjić, M. Todorović, M. Trtanj, Y. Pogozhev, Y. Blagoveschenskii, E. A. Levashov, *Colloids Surfaces, A* **297** (2007) 1
26. S. H. Gregg, K. S. Sing, *Adsorption, Surface Area and Porosity*, Academic Press, New York, 1982, p. 41
27. F. Rouquerol, J. Rouquerol, K. Sing, *Adsorption by powders and porous solids*, Academic Press, London, 1999, p. 440
28. P. A. Webb, C. Orr, *Analytical methods in fine particle technology*, Micromeritics Instrument Corporation, Norcross, GA, 1997, p. 53
29. S. J. Chipera, D. L. Bish, *Clay Clay Miner.* **49** (2001) 398
30. T. Hayakawa, M. Minase, K. I. Ujita, M. Ogawa , *Clay Clay Miner.* **64** (2016) 275
31. P. Cañizares, J. L. Valverde, M. R. Sun Kou, C. B. Molina, *Micropor. Mesopor. Mat.* **29** (1999) 267
32. G. Leofanti, M. Padovan, G. Tozzola, B. Venturelli, *Catal. Today* **41** (1998) 207
33. N. Jović-Jovičić, A. Milutinović-Nikolić, M. Žunić, Z. Mojović, P. Bankovića, I. Gržetić, D. Jovanović, *J. Contam. Hydrol.* **150** (2013) 1
34. Z. Sandić, A. Nastasović, N. Jović-Jovičić, A. Milutinović-Nikolić, D. Jovanović, *Appl. Polym. Sci.* **121** (2011) 234
35. S. Lagergren, *K. Vet. Akad. Handl.* **24** (1898) 1
36. Y. S. Ho, G. McKay, *Chem. Eng. J.* **70** (2) (1998) 115
37. I. J. Langmuir, *J. Am. Chem. Soc.* **40** (1918) 1361
38. H. M. F. Freundlich, *J. Phys. Chem.* **57** (1906) 385
39. M. M. Dubinin, L. V. Radushkevich, *Chem Zent*. **1** (1947) 875.
40. M. Horsfall, A. I. Spiff, A. A. Abia, *Bull. Kor. Chem. Soc.* **25** (2004) 969
41. C. Y. Abasi, A. A. Abia, J. C. Igwe, *Envron. Res. J.* **5** (2011) 104.